



Contents lists available at ScienceDirect

## Journal of Quantitative Spectroscopy and Radiative Transfer

journal homepage: [www.elsevier.com/locate/jqsrt](http://www.elsevier.com/locate/jqsrt)

Review

Measurements of H<sub>2</sub>O broadened by CO<sub>2</sub> line-shape parameters: Beyond the Voigt profileÉ. Ducreux<sup>a,b,c</sup>, B. Grouiez<sup>a</sup>, S. Robert<sup>b</sup>, M. Lepère<sup>c</sup>, B. Vispoel<sup>c</sup>, R.R. Gamache<sup>d</sup>, L. Régalia<sup>a,\*</sup><sup>a</sup> Université de Reims Champagne-Ardenne, CNRS, GSMA, Reims, France<sup>b</sup> Planetary Atmospheres, Royal Belgian Institute for Space Aeronomy, 3 Avenue Circulaire, 1180 Brussels, Belgium<sup>c</sup> Research Unit Lasers and Spectroscopies (LLS), Institute of Life, Earth and Environment (ILEE), University of Namur (UNamur), 61 rue de Bruxelles, Namur 5000, Belgium<sup>d</sup> Department of Environmental, Earth, and Atmospheric Sciences, University of Massachusetts Lowell, 1 University Avenue, Lowell, MA 01854, USA

## ARTICLE INFO

## Keywords:

High resolution infrared spectroscopy

Line shape parameters

Water vapor

Carbon dioxide

Line profiles

Planetary atmospheres

## ABSTRACT

H<sub>2</sub>O is an important molecule in the quest to better understand the evolution of solar system. In the study of Venus and Mars CO<sub>2</sub>-rich atmospheres (around 96 % of their composition) and because of the space instruments constant improvements, the planetary community needs spectroscopic data as accurate as possible.

Continuing from our previous study [JQSRT 231, 126(2019)], new spectra of H<sub>2</sub>O perturbed by CO<sub>2</sub> were measured with our new experimental set-up in the 2.7 μm region to compare with the previous results. After the improvement in the determination of the partial pressure of water vapor, the line parameters were then determined with a multispectrum fitting procedure using a Voigt profile in the same way as in [JQSRT 231, 126 (2019)]. This led to characteristic W-shape residuals that have been improved using beyond-Voigt profiles. Our investigation showed that considering the speed dependence of collisional line parameters is essential to obtain better line-shape parameters in the considered experimental conditions.

## 1. Introduction

As part of the study of our solar system evolution and research on terrestrial water's origins, it is particularly important to know the distribution of water vapor and its isotopologues in the atmosphere of our planetary neighbors, Venus and Mars. Venus Express (2008–2014) and ExoMars Trace Gas Orbiter (2016–), both ESA missions and also ground-based measurements have mapped water [1–7]. From these measurements, the isotopic ratio, deuterium to hydrogen, D/H, has been deduced to constrain atmospheric evolution scenarios [8–11].

Until recently, collisional parameters of H<sub>2</sub>O broadened by air were used due to lack of data instead of H<sub>2</sub>O broadened by CO<sub>2</sub> line collisional parameters in planetary spectrum analysis. It was therefore essential to provide the planetary science community with measurements of H<sub>2</sub>O broadened by CO<sub>2</sub> line-shape parameters in several regions of atmospheric interest. Some studies have already contributed to the determination of these collisional parameters [12–20] for H<sub>2</sub>O and [21–24] for HDO. Note, to our knowledge, CO<sub>2</sub>-broadening parameters of D<sub>2</sub>O have never been measured. Among these studies, Ref. [12] presented spectra recorded in the 2.7 and 6 μm regions with a step-by-step Connes'

type Fourier-Transform spectrometer (FTS) and analyzed with a Voigt profile. More recently new spectra were measured in the 2.7 μm region with a Bruker IFS 125 HR FTS coupled to a 2-m White-type cell. The pressure of water vapor was kept sufficiently low to avoid self-broadening contribution, as was already done in our previous study [12]. As water vapor is a polar molecule, it is well-known that the sample adsorption must be considered. So, the H<sub>2</sub>O partial pressure needs to be determined precisely. The differences between observations and the modeling (i.e. the residuals) showed that the partial pressure of water vapor in the experiment may not have been considered properly. Another gas injection method was tested. In [12], an initial mixture of H<sub>2</sub>O – CO<sub>2</sub> was injected in the cell and one spectrum was measured after each pumping. Whereas in this work, after the injection of a low pressure of water vapor, the CO<sub>2</sub> was injected gradually, and a spectrum was recorded after each new mixture. The analysis of these new measurements required to go beyond the Voigt profile. Using this common profile led to W-shape residuals due to a narrowing effect. More complex line profiles were investigated to obtain more accurate collisional line parameters.

Section 2 describes the experimental setup and the method for line

\* Corresponding author.

E-mail address: [laurence.regalia@univ-reims.fr](mailto:laurence.regalia@univ-reims.fr) (L. Régalia).<https://doi.org/10.1016/j.jqsrt.2024.109026>

Received 20 February 2024; Received in revised form 19 April 2024; Accepted 23 April 2024

Available online 26 April 2024

0022-4073/© 2024 Elsevier Ltd. All rights reserved.

parameters' retrieval. Section 3 is dedicated to comparisons and results.

## 2. Experimental conditions

### 2.1. Spectra measurements

A FTS, commercial Bruker IFS 125 HR, was used to measure water vapor broadened by carbon dioxide spectra in the 2.7  $\mu\text{m}$  region at room temperature. The wavelength range was selected to be able to compare to previous measurements [12]. The characteristics of the FTS are listed in Table 1. During the experiment, a primary oil pump and a turbomolecular secondary pump maintained the absorption path under vacuum - around  $5.10^{-5}$  mbar - to reduce residual background water.

A 2-m White-type cell in stainless-steel was combined with the spectrometer to reach absorption path lengths from 8 to 104 m.

For the cell pressure monitoring, three thermalized Leybold CTR101N Baratron gauges heads with a range of respectively 10, 100 and 1000 Torr were used, coupled with a conversion box for pressure reading. They have an accuracy of 0.2 % and are calibrated beforehand. Temperatures were measured in the cell by four TCSA Pt100 probes with 0.6 K of accuracy, coupled with a Meilhaus Electronics conversion box.

Experimental conditions are given in Table 2 for a series of spectra shown in Fig. 1. The partial pressure of  $\text{H}_2\text{O}$  was 1.465 Torr. Within these conditions, line intensities from  $4.10^{-21}$  to  $1.10^{-23}$   $\text{cm}^{-1}$  / (molecule  $\text{cm}^{-2}$ ) were measured in the 2.7  $\mu\text{m}$  region, choosing to analyze lines ranging from 15 to 80 % of absorption. As seen in Fig. 1, by increasing the partial pressure of  $\text{CO}_2$  in the cell, the water vapor lines were increasingly broadened, hence the maximum path difference (MPD) was reduced (see Table 2) to maintain a good signal to noise ratio with a shorter measurement duration. This led to reach a mean signal to noise ratio around 3500, determined with Bruker's software Opus by selecting several spectral intervals without visible lines. The  $\text{CO}_2$  gas was purchased from Air Liquid with a stated purity ( $\text{CO}_2$  N48) of 99.998 %. The gas injection method is discussed in Section 2.2.1.

### 2.2. Line parameters retrieval

A multispectrum fitting procedure was used to determine collisional parameters of  $\text{H}_2\text{O}$  broadened by  $\text{CO}_2$  lines. Two software packages were used complementarily. The first one called MultiFit [25] - MFT - was developed in-house. The second one called MultiSpectrum Fitting - MSF - is described in [26]. Both can fit simultaneously several parameters, such as position, intensity, broadening and shift coefficients, but only MFT enables one to fit the partial pressure. However, MSF is not limited to the Voigt profile and offers more complex line profiles.

The analysis was carried out only on isolated lines with an absorption between 15 % and 80 % to ensure well defined parameters without any saturation effect.

#### 2.2.1. Gas mixture

Using both the MFT [25] and MSF [26] software with the Voigt profile on absorption lines, signatures on observed - calculated residuals as shown on Fig. 2 (left panel) were observed. This type of residuals

**Table 2**

Experimental conditions of the four  $\text{H}_2\text{O}$  -  $\text{CO}_2$  spectra for the 2.7  $\mu\text{m}$  region. The path length was 826.2 cm, and the aperture radius was 0.85 mm.

Total pressure [Torr]	MPD [cm]	Spectral resolution [ $\text{cm}^{-1}$ ]	Temperature [K]
99.4	56.25	0.016	291.8
200.4	50.00	0.018	291.7
300.1	45.00	0.020	291.8
500.6	40.90	0.022	291.8

differs from the typical W-shape signature generally induced by an inadequate line profile. In our case, the residuals are off-centered suggesting an uncertainty on the water vapor partial pressure. This possibility was investigated and developed further in the next sections.

First, the water vapor was produced by pumping over a sample of liquid water in natural abundance. The use of a static setup for water is quite tricky.  $\text{H}_2\text{O}$  being a polar molecule, it can easily stick on stainless-steel cell walls, because of the adsorption effect. That is why our partial pressure does not correspond to the pressure injected. Therefore, the way the gas mixture is injected will have an impact on the spectra. Indeed, in Ref [12], the water vapor was injected, before adding a single 500 Torr pressure of  $\text{CO}_2$  in the cell. The mixture was then pumped to reach lower pressures. So, the partial pressure of  $\text{H}_2\text{O}$  was different for each spectrum.

For this work, the procedure of gas injection was modified to have the same  $\text{H}_2\text{O}$  partial pressure for each spectrum of a series. Before each new recording, adequate time was taken to allow the mixture to become homogeneous and the pressure to stabilize. With this method, the pressure of  $\text{H}_2\text{O}$  was stable, whereas the mixing ratio changed radically between the four spectra (see Table 3).

As our experimental gas injection facility is static and not based on a constant flow that avoids the sticking of water molecules to cell walls [27], a post-correction of the water vapor partial pressure needs to be performed to take into account adsorption [28]. It was then necessary to better determine the  $\text{H}_2\text{O}$  partial pressure to obtain the best fit residuals and line parameters. Our method consisted in fitting the  $\text{H}_2\text{O}$  partial pressure with the MFT software [25] by fixing the intensity values at those of HITRAN2020 [29] on 14 isolated lines. Among these, eleven lines have a relative uncertainty of less than 1 %, while the three others have a relative uncertainty between 2 % and 5 %. This results in a maximum relative uncertainty of approximately 1.9 % (weighted mean) for the selected intensities.

It was found that for the 100, 200 and 300 Torr spectra, the fitted  $\text{H}_2\text{O}$  partial pressure was always around 3 % lower than the measured one, as seen in Table 3. For the 500 Torr spectrum, the fitted pressure had an aberrant value probably coming from the large broadening of the lines and which did not allow convergence to a coherent fitted pressure value. Thus, by considering that the deviation remained constant, the mean of the three first  $\text{H}_2\text{O}$  partial pressures was used for the 500 Torr spectrum. Fig. 2 (right panel) shows a finer improvement of the residuals and clear W-shape signature due to the use of an inappropriate profile.

#### 2.2.2. Line profiles and collisional line parameters

The common profile used to fit spectral lines and provided to spectroscopic databases is the Voigt profile (VP) [30], but several studies [31–34] (non-exhaustive list) have already shown that it is not the most suitable for  $\text{H}_2\text{O}$  studies and that it usually can bring a W-shape in the fit residuals coming from a narrowing of the line. To correctly model the lines, other more elaborate line profiles were developed that include physical mechanisms of broadening. The MSF software [26] allows the use of the Rautian profile (RP) [35], the quadratic Speed-Dependent Voigt profile (qSDVP) [36–41] and the quadratic Speed-Dependent Rautian profile (qSDRP) [42]. The VP, RP and qSDVP are limiting cases of the qSDRP [43,44], as shown in Table 4.

The Rautian profile takes into account the Dicke narrowing effect

**Table 1**

Experimental conditions for the FT-IR spectrometer for measurements in 2.7  $\mu\text{m}$  region, i.e. around  $3704$   $\text{cm}^{-1}$ .

Source	Glober SiC
Tension	24 V
Intensity	3.28 A
Iris radius	0.85 mm
Focal length	41.8 cm
Modulation frequency	40 kHz
Optical filter	Band pass 3060–4370 $\text{cm}^{-1}$
Beam splitter	$\text{CaF}_2$
Detector	InSb, 77 K

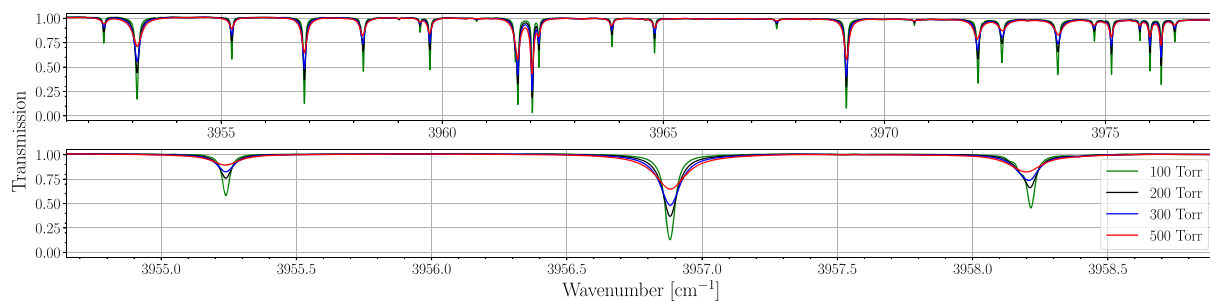


Fig. 1. Example of H<sub>2</sub>O broadened by CO<sub>2</sub> spectra in 2.7 μm region, with a zoom around 3957 cm<sup>-1</sup>.

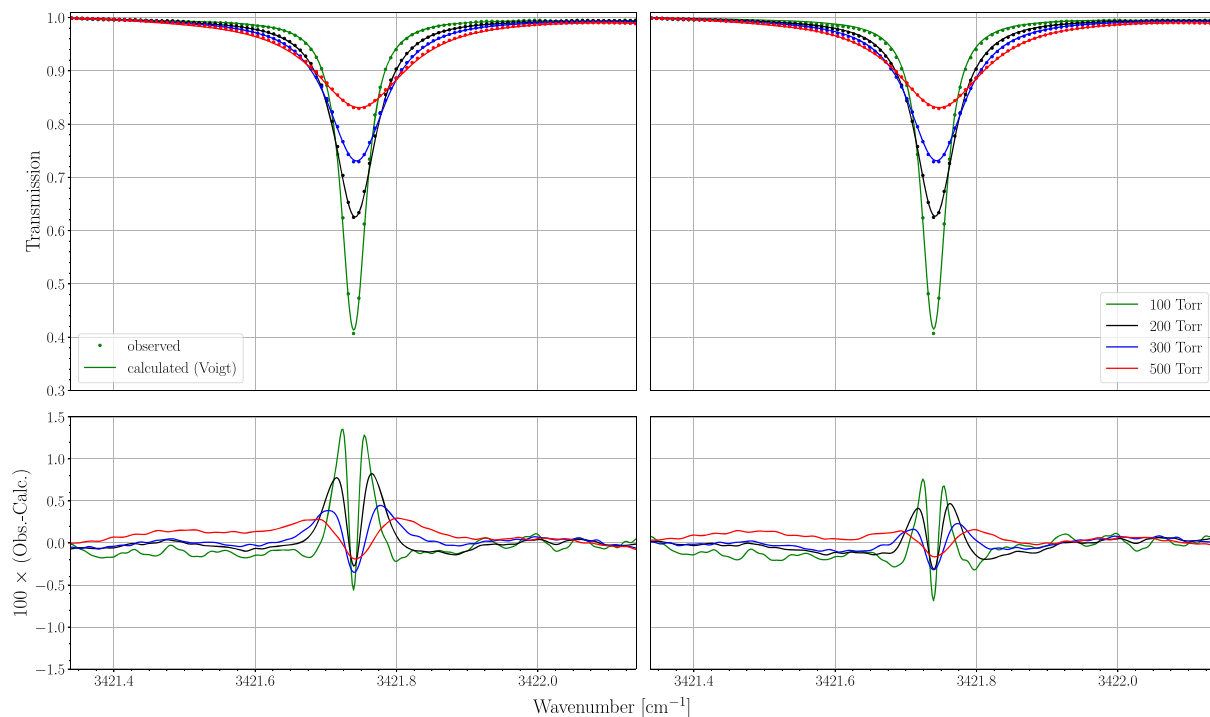


Fig. 2. Fit residuals without (left panel) and with (right panel) water vapor partial pressure correction (Table 3) for one transition centered at 3421.74 cm<sup>-1</sup> using a Voigt profile.

Table 3

Comparison between measured and fitted H<sub>2</sub>O partial pressures of H<sub>2</sub>O – CO<sub>2</sub> spectra for the “injection” series in 2.7 μm region. The relative deviation was calculated as follows (fitted pressure - measured pressure)/measured pressure.

Total pressure [Torr]	Measured P(H <sub>2</sub> O) [Torr]	Fitted P(H <sub>2</sub> O) [Torr]	Relative deviation
99.4	1.465	1.422	-2.9 %
200.4	1.465	1.419	-3.1 %
300.1	1.465	1.421	-3.0 %
500.6	1.465	1.421	-3.0 %

[45] due to collision-induced velocity changes in the case of hard collisions. In this model, active light molecules are colliding in a heavy molecule environment at a pressure sufficiently low that the Maxwell-Boltzmann distribution is not maintained. Each new collision causes a speed change, independent of the initial speed of the molecule. And because it is more likely that a molecule will lose speed after a collision rather than gain it, the Doppler shift decreases and the line narrows.

The quadratic speed-dependent Voigt profile allows to consider the speed dependences of the line width and shift (Eq. 1) [43] by taking into

Table 4

Profiles used for the H<sub>2</sub>O – CO<sub>2</sub> collision system. The parameters are described as follows:  $\Gamma_0$  the pressure-induced broadening coefficient (cm<sup>-1</sup>.atm<sup>-1</sup>),  $\Delta_0$  the pressure-induced shift coefficient (cm<sup>-1</sup>.atm<sup>-1</sup>),  $\Gamma_2$  the speed-dependence of the pressure-induced broadening coefficient (cm<sup>-1</sup>.atm<sup>-1</sup>),  $\Delta_2$  the speed-dependence of the pressure-induced shift coefficient (cm<sup>-1</sup>.atm<sup>-1</sup>),  $\nu_{VC}$  the frequency rate of velocity-changing collisions (cm<sup>-1</sup>.atm<sup>-1</sup>).

Profile	Parameters
VP	$\Gamma_0, \Delta_0$
RP	$\Gamma_0, \Delta_0, \nu_{VC}$
qSDVP	$\Gamma_0, \Delta_0, \Gamma_2, \Delta_2$
qSDRP	$\Gamma_0, \Delta_0, \Gamma_2, \Delta_2, \nu_{VC}$

account the relative speed between the absorbing and the perturbing molecules, which leads to a narrowing and an asymmetry of the line.

$$\begin{cases} \Gamma(\nu) = \Gamma_0 + \Gamma_2 \left[ \left( \frac{\nu}{\nu_p} \right)^2 - \frac{3}{2} \right] \\ \Delta(\nu) = \Delta_0 + \Delta_2 \left[ \left( \frac{\nu}{\nu_p} \right)^2 - \frac{3}{2} \right] \end{cases} \quad (1)$$

$\Gamma_0$  and  $\Delta_0$  are respectively the averaged values over all molecular speed  $\nu$  of the line collisional width and shift.  $\Gamma_2$  and  $\Delta_2$  are respectively the quadratic speed dependence of the line collisional width and shift.  $\nu_p = \sqrt{2k_B T/m}$  is the most probable speed at temperature  $T$  of the active molecule of mass  $m$ .

The quadratic dependence model [38,39] is a good approximation allowing a relatively short time of numerical computation.

Finally, the quadratic speed-dependent Rautian profile is a combination of two profiles mentioned above considering the confinement narrowing effect and the speed dependence of the broadening and shift coefficients. It results in a longer calculation time compared to that of the qSDV profile.

### 3. Results and discussion

In this section, the results obtained with the four spectra of the series given in Table 2 were presented. As the partial pressure of H<sub>2</sub>O was previously determined (see previous section) with the MFT program [25], the line intensity was fixed during the fitting procedure; the position, the CO<sub>2</sub> broadening and shift coefficients were adjusted. The following results were obtained using the MSF software [26].

#### 3.1. Comparisons using Voigt profile

First, in Fig. 3 the CO<sub>2</sub> broadening coefficients coming from our previous study [12] were compared with those obtained in this work (called “S2023” from now on), all determined with the Voigt profile. Followed mean relative deviations were found: 2.8 % between the experimental coefficients from spectra recorded in 2023 with and without water vapor pressure correction and 2.3 % between the experimental coefficients from [12] and S2023 with pressure correction. Between MCRB calculations provided in [12] and S2023 with pressure correction, only 2.0 % were obtained against 4.1 in [12] for the same selected lines. So, making a correction to the water vapor partial pressure helped to obtain a better agreement between the experiments and the calculations. The plot was made with respect to the index  $J''^* (J''+1)+Ka''-Kc''+1$ , which is unique for each line.

#### 3.2. Line profile comparisons

After the correction of the water vapor partial pressure on our spectra, there remained a W-shape on our residuals, typical of the Voigt profile model (Fig. 2, right panel). To go beyond, more complex line profiles, described above, were used: the Rautian profile, the quadratic Speed-Dependent Voigt profile and the quadratic Speed-Dependent Rautian profile. An example of the fit residuals obtained using the four different line profiles is shown in Fig. 4.

Considering firstly the Dicke narrowing effect using the Rautian profile, Fig. 4 shows that it did not bring significant improvement. In contrast, the residuals are really improved by a factor of at least five if the speed-dependence on CO<sub>2</sub> broadening and CO<sub>2</sub> pressure-induced shift coefficients are considered using the quadratic Speed-Dependent Voigt profile. The W-shape, previously visible, was greatly diminished. Using quadratic Speed-Dependent Rautian profile led to residuals like

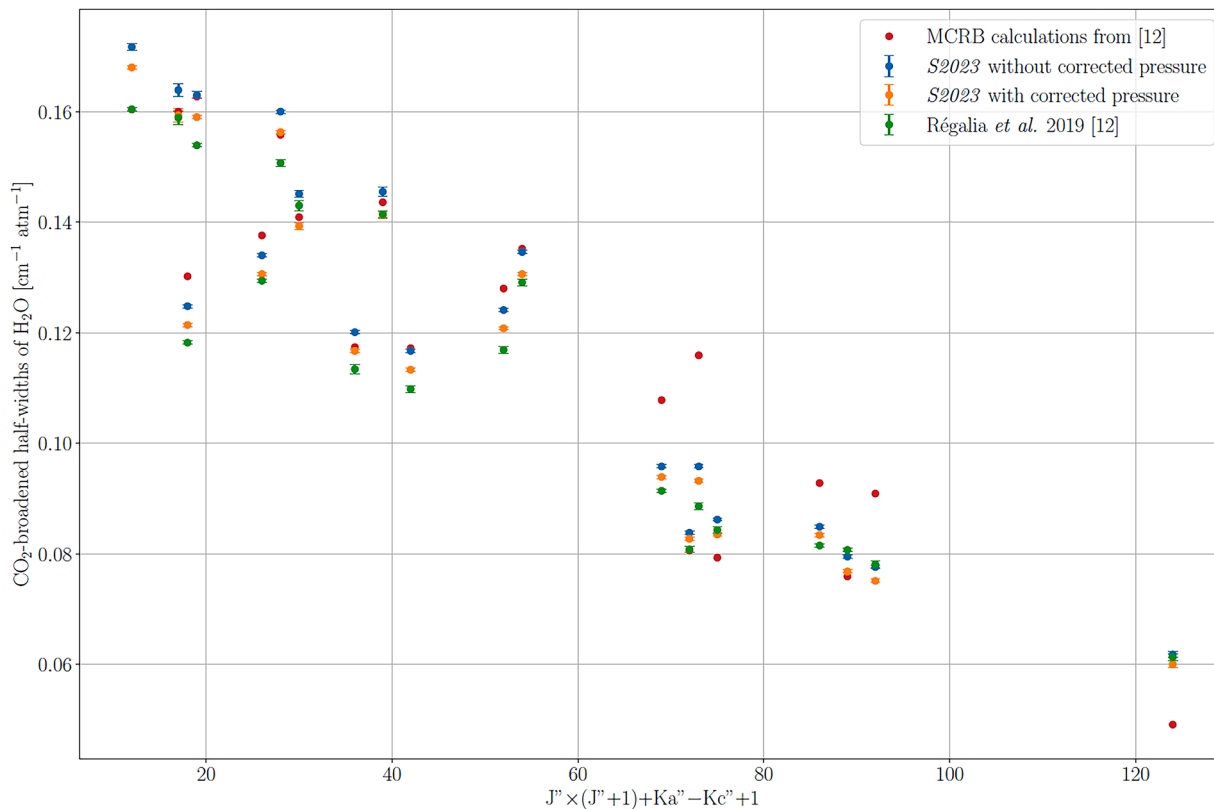


Fig. 3. Comparison for 20  $\nu_3$  transitions of experimental CO<sub>2</sub> broadening coefficients from [12] and MCRB calculations performed for our previous study [12] with S2023 using a Voigt profile with and without the water vapor partial pressure correction. The uncertainties are the numerical errors provided by the multi-spectrum fitting procedure at 3-sigma.

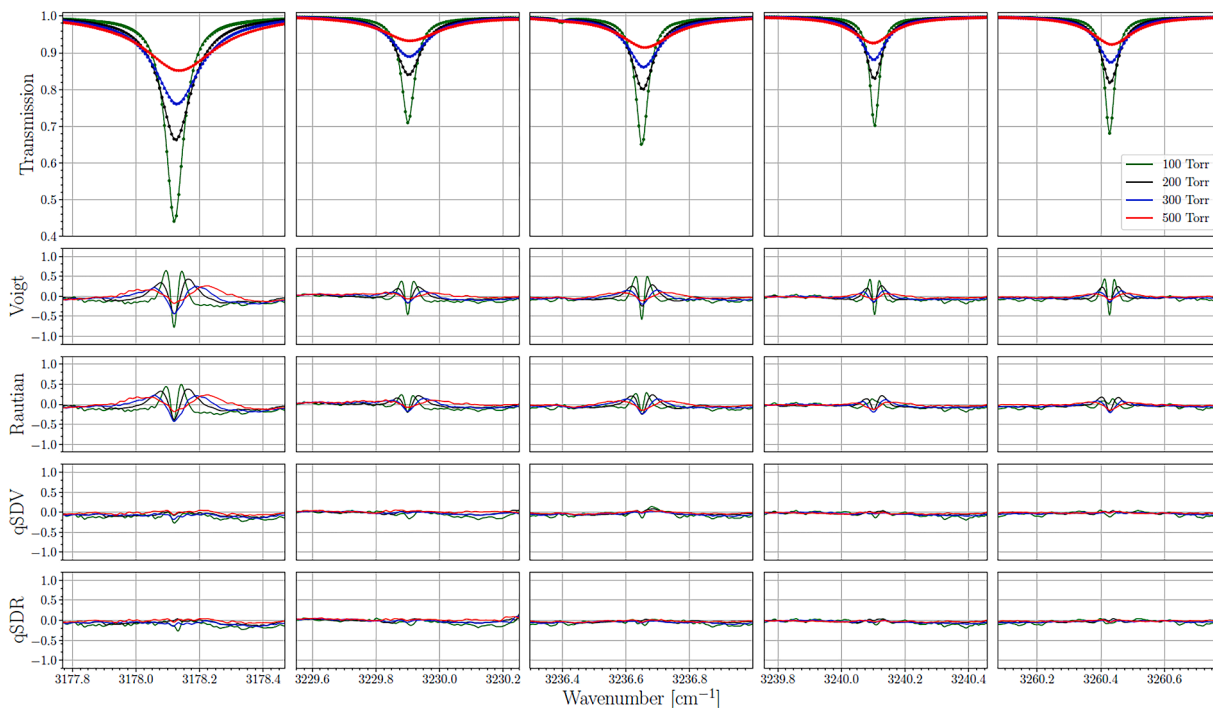


Fig. 4. Example in 2.7  $\mu\text{m}$  region of  $\text{H}_2\text{O}$  broadened by  $\text{CO}_2$  spectra fits using different line profiles and their 100x (Obs.-Calc.) residuals.

those obtained with the qSDVP.

The quadratic Speed-Dependent Voigt and the quadratic Speed-Dependent Rautian profiles were more suitable than the other models to obtain very low residuals. And because the first had a lower computation time and a lower number of parameter than the second for similar results, the quadratic Speed-Dependent Voigt profile seems to be in the considered experimental conditions, the best choice in the analysis of  $\text{H}_2\text{O}$  broadened by  $\text{CO}_2$  lines.

### 3.3. Literature comparison

By comparing our  $\text{CO}_2$  broadening coefficient measurements obtained with the quadratic Speed-Dependent Voigt profile with those obtained with the Voigt profile, a mean relative deviation of approximately 4.1 % has been found for 78 transitions in  $\nu_1$ ,  $2\nu_2$  and  $\nu_3$  bands. A similar observation was done in [17], where the broadening with the quadratic speed-dependent Voigt profile was found higher of 4.7 % for  $\nu_1 + 2\nu_2 + \nu_3$ ,  $2\nu_1 + \nu_3$  and  $3\nu_1$  bands, than broadening with the Voigt profile.

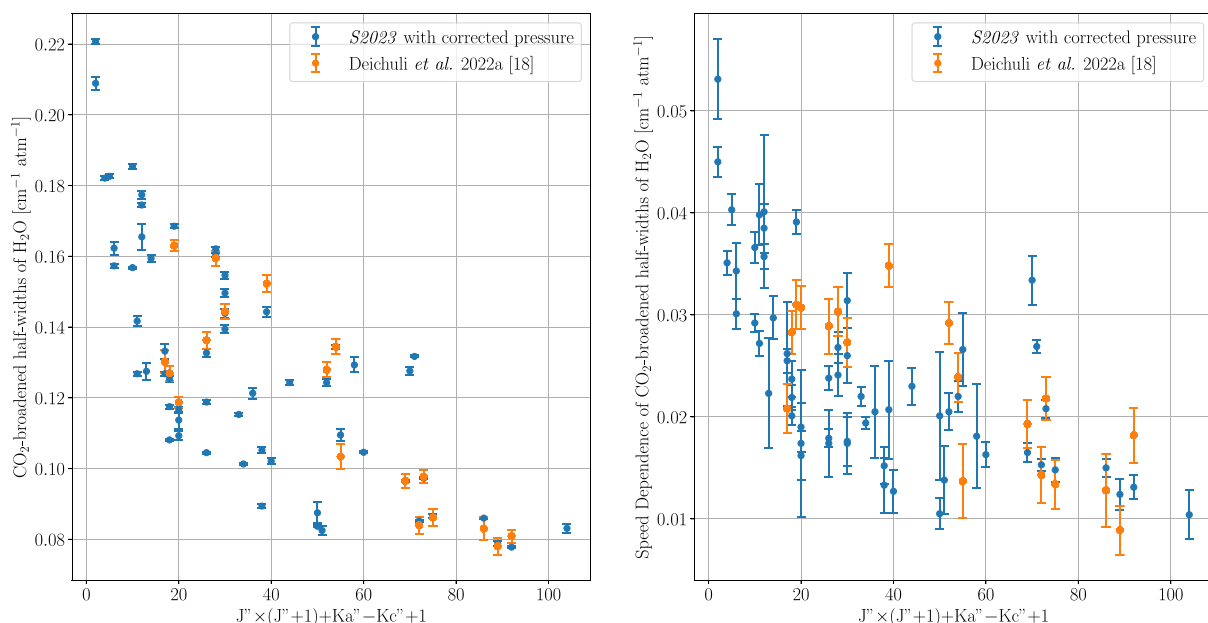


Fig. 5. Comparison between our  $\text{CO}_2$  broadening coefficients and their speed dependence (*S2023* with  $\text{H}_2\text{O}$  partial pressure correction) with those of Deichuli et al., 2022a [18]. The uncertainties came from numerical errors provided by the multi-spectrum fitting procedure at 3-sigma.

In the literature, the only study at 2.7  $\mu\text{m}$  using a profile considering the speed is the work of Deichuli et al. [18]. Since in our study, a cell with a longer path length was used (8 m compared to 24 cm), these two studies did not have access to the same transitions. However, 18 lines were common with our measurements and comparisons are presented in Fig. 5. The mean relative deviation for CO<sub>2</sub> broadening coefficients and their speed dependence was found of, respectively of 0.6 % and 15.3 %. So, a good agreement was found for the first parameter and quite far for the second one with no clear explanations. Nevertheless, it was not surprising given that the speed dependence coefficients are difficult to determine. Note that in [18], the speed-dependence of the shift induced by the CO<sub>2</sub> pressure was fixed to zero whereas it was not the case in this work. By using the same configuration in our study, the mean relative deviations for CO<sub>2</sub> broadening coefficients and their speed dependence are larger, respectively 1.3 % and 33.6 %.

#### 4. Conclusions

An IFS 125 HR Bruker Fourier-Transform spectrometer was used to measure spectra of H<sub>2</sub>O broadened by CO<sub>2</sub> in the 2.7  $\mu\text{m}$  spectral region of atmospheric interest. A multispectrum fitting procedure was used to better determine the water vapor partial pressure. The line-shape parameters were determined with several line profiles: Voigt profile, Rautian profile, quadratic speed-dependent Voigt profile and quadratic speed-dependent Rautian profile and their fit residuals compared. The quadratic speed-dependent Voigt profile was the more appropriate line profile to fit H<sub>2</sub>O broadened by CO<sub>2</sub> spectral lines yielding low residuals. This work is a part of an ambitious investigation aiming at preparing future space missions. Spectral regions of interest for Ariel [46,47] and EnVision [48], for instance, will be studied.

#### CRedit authorship contribution statement

**É. Ducreux:** Writing – original draft, Methodology, Formal analysis, Data curation. **B. Grouiez:** Methodology, Data curation. **S. Robert:** Writing – original draft, Validation, Supervision. **M. Lepère:** Validation, Supervision. **B. Vispoel:** Writing – review & editing. **R.R. Gamache:** Writing – review & editing. **L. Régalia:** Writing – original draft, Validation, Supervision, Methodology, Formal analysis.

#### Declaration of competing interest

The authors declare that they have no known competing financial interests or personal relationships that could have appeared to influence the work reported in this paper.

#### Data availability

Data will be made available on request.

#### Acknowledgments

This work was supported by the Programme National de Planétologie (PNP) of CNRS-INSU co-funded by CNES. S.R. acknowledges funding by the Belgian Science Policy Office (BELSPO) through the FED-tWIN program (Prf-2019-077 - RT-MOLEXO) and through financial and contractual support coordinated by the ESA Prodex Office (PEA 4000137943, 4000128137). B.V. would like to thank the F.R.S.-FNRS for postdoctoral financial support. The authors sincerely thank Dr K. Sung from Jet Propulsion Laboratory in California (USA) for many useful discussions, his expertise and advice on pressure measurements of water vapor.

#### References

- [1] de Bergh C, Bézard B, Crisp D, Maillard JP, Owen T, Pollack J, Grinspoon DH. Water in the deep atmosphere of Venus from high-resolution spectra of the night side. *Adv Space Res* 1995;15:79–88. [https://doi.org/10.1016/0273-1177\(94\)00067-B](https://doi.org/10.1016/0273-1177(94)00067-B).
- [2] Fedorova A, Korablev O, Vandaele AC, Bertaux J-L, Belyaev D, Mahieux A, Neefs E, Wilquet WV, Drummond R, Montmessin F, Villard E. HDO and H<sub>2</sub>O vertical distributions and isotopic ratio in the Venus mesosphere by Solar Occultation at Infrared spectrometer on board Venus Express. *J Geophys Res* 2008;113:E00B22. <https://doi.org/10.1029/2008JE003146>.
- [3] Krasnopolsky VA, Belyaev DA, Gordon IE, Li G, Rothman LS. Observations of D/H ratios in H<sub>2</sub>O, HCl, and HF on Venus and new DCl and DF line strengths. *Icarus* 2013;224:57. <https://doi.org/10.1016/j.icarus.2013.02.010>.
- [4] Aoki S, Vandaele AC, Daerden F, Villanueva GL, Liuzzi G, Thomas IR, Erwin JT, Trompet L, Robert S, Neary L, Viscardy S, Clancy RT, Smith MD, Lopez-Valverde MA, Hill B, Ristic B, Patel MR, Bellucci G, Lopez-Moreno J-J. Water vapor vertical profiles on Mars in dust storms observed by TGO/NOMAD. *J Geophys Res: Planets* 2019;124(12):3482–97. <https://doi.org/10.1029/2019JE006109>.
- [5] Crismani MMJ, Villanueva GL, Liuzzi G, Smith MD, Knutsen EW, Daerden F, Neary L, Mumma MJ, Aoki S, Trompet L, Thomas IR, Ristic B, Bellucci G, Piccialli A, Robert S, Mahieux A, Lopez Moreno J-J, Sindoni G, Giuranna M, Patel MR, Vandaele AC. A global and seasonal perspective of Martian water vapor from ExoMars/NOMAD. *J Geophys Res: Planets* 2021;126(11):e2021JE006878. <https://doi.org/10.1029/2021JE006878>.
- [6] Aoki S, Vandaele AC, Daerden F, Villanueva GL, Liuzzi G, Clancy RT, Lopez-Valverde MA, Brines A, Thomas IR, Trompet L, Erwin JT, Neary L, Robert S, Piccialli A, Holmes JA, Patel MR, Yoshida N, Whiteway J, Smith MD, Ristic B, Bellucci G, Lopez-Moreno JJ, Fedorova AA. Global vertical distribution of water vapor on Mars: results from 3.5 years of ExoMars-TGO/NOMAD science operations. *J Geophys Res: Planets* 2022;127(9):e2022JE007231. <https://doi.org/10.1029/2022JE007231>.
- [7] Mahieux A, Robert S, Piccialli A, Trompet L, Vandaele AC. The SOIR/Venus Express species concentration and temperature database: CO<sub>2</sub>, CO, H<sub>2</sub>O, H<sup>35</sup>Cl, H<sup>37</sup>Cl, HF individual and mean profiles. *Icarus* 2023;405(A115713). <https://doi.org/10.1016/j.icarus.2023.115713>.
- [8] Villanueva GL, Mumma MJ, Novak RE, Käufel HU, Hartogh P, Encrenaz T, Tokunaga A, Khayat A, Smith MD. Strong water isotopic anomalies in the Martian atmosphere: probing current and ancient reservoirs. *Science* 2015;348(6231):218–21. <https://doi.org/10.1126/science.aaa3630>.
- [9] Vandaele AC, Korablev O, Daerden F, Aoki S, Thomas IR, Altieri F, Rodionov D. Martian dust storm impact on atmospheric H<sub>2</sub>O and D/H observed by ExoMars trace gas orbiter. *Nature* 2019;568(7753):521–5. <https://doi.org/10.1038/s41586-019-1097-3>.
- [10] Villanueva GL, Liuzzi G, Aoki S, Stone SW, Brines A, Thomas IR, Vandaele AC. The deuterium isotopic ratio of water released from the Martian caps as measured with TGO/NOMAD. *Geophys Res Lett* 2022;49(12):e2022GL098161. <https://doi.org/10.1029/2022GL098161>.
- [11] Mahieux, et al. Unexpected increase of the deuterium to hydrogen ratio in the Venus mesosphere. *PNAS*; 2024. in revision.
- [12] Régalia L, Cousin E, Gamache RR, Vispoel B, Robert S, Thomas X. Laboratory measurements and calculations of line shape parameters of the H<sub>2</sub>O–CO<sub>2</sub> collision system. *J Quant Spectrosc Radiat Transf* 2019;231:126–35. <https://doi.org/10.1016/j.jqsrt.2019.04.012>.
- [13] Gamache RR, Neshyba SP, Plateaux JJ, Barbe A, Régalia L, Pollack JB. CO<sub>2</sub>-broadening of water-vapor lines. *J Mol Spectrosc* 1995;170:131–51. <https://doi.org/10.1006/jmsp.1995.1060>.
- [14] Brown LR, Humphrey CM, Gamache RR. CO<sub>2</sub>-broadened water in the pure rotation and  $\nu_2$  fundamental regions. *J Mol Spectrosc* 2007;246:1–21. <https://doi.org/10.1016/j.jms.2007.07.010>.
- [15] Lavrentieva NN, Voronin BA, Fedorova AA. H<sub>2</sub><sup>18</sup>O line list for the study of atmospheres of Venus and Mars. *Opt Spectrosc* 2015;118:11–8. <https://doi.org/10.1134/S0030400X15010178>.
- [16] Gamache RR, Faresse M, Renaud CL. A spectral line list for water isotopologues in the 1100–4100 cm<sup>-1</sup> region for application to CO<sub>2</sub>-rich planetary atmospheres. *J Mol Spectrosc* 2016;326(1):144–50. <https://doi.org/10.1016/j.jms.2015.09.001>. New Visions of Spectroscopic Databases.
- [17] Borkov YG, Petrova TM, Solodov AM, Solodov AA. Measurements of the broadening and shift parameters of the water vapor spectral lines in the 10,100–10,800 cm<sup>-1</sup> region induced by pressure of carbon dioxide. *J Mol Spectrosc* 2018;344:39–45. <https://doi.org/10.1016/j.jms.2017.10.010>.
- [18] Deichuli VM, Petrova TM, Solodov AA, Solodov AM. Broadening and shift coefficients of water absorption lines induced by carbon dioxide pressure near 2.7  $\mu\text{m}$ . *Atmos Ocean Opt* 2022;35:634–8. <https://doi.org/10.1134/S1024856022060070>.
- [19] Deichuli VM, Petrova TM, Solodov AM, Solodov AA, Fedorova AA. Water vapor absorption line parameters in the 6760–7430 cm<sup>-1</sup> region for application to CO<sub>2</sub>-rich planetary atmosphere. *J Quant Spectrosc Radiat Transf* 2022;293:108386. <https://doi.org/10.1016/j.jqsrt.2022.108386>.
- [20] Petrova TM, Solodov AM, Solodov AA, Deichuli VM, Lavrent'eva NN, Dudaryonok AS. Measurements and calculations of CO<sub>2</sub>-broadening and shift coefficients of water vapor transitions in the 5150–5550 cm<sup>-1</sup> spectral region. *J Quant Spectrosc Radiat Transf* 2023;311:108757. <https://doi.org/10.1016/j.jqsrt.2023.108757>.
- [21] Devi VM, Benner DC, Sung K, Crawford TJ, Gamache RR, Renaud CL, Smith M-AH, Mantz AW, Villanueva GL. Line parameters for CO<sub>2</sub> broadening in the  $\nu_2$  band of

- HD<sub>16</sub>O. *J Quant Spectrosc Radiat Transf* 2017;187:472–88. <https://doi.org/10.1016/j.jqsrt.2016.10.004>.
- [22] Devi VM, Benner DC, Sung K, Crawford TJ, Gamache RR, Renaud CL, Smith M-AH, Mantz AW, Villanueva GL. Line parameters for CO<sub>2</sub>- and self-broadening in the  $\nu_1$  band of HD<sub>16</sub>O. *J Quant Spectrosc Radiat Transf* 2017;203:133–57. <https://doi.org/10.1016/j.jqsrt.2017.01.032>.
- [23] Devi VM, Benner DC, Sung K, Crawford TJ, Gamache RR, Renaud CL, Smith M-AH, Mantz AW, Villanueva GL. Line parameters for CO<sub>2</sub>- and self-broadening in the  $\nu_3$  band of HD<sub>16</sub>O. *J Quant Spectrosc Radiat Transf* 2017;203:158–74. <https://doi.org/10.1016/j.jqsrt.2017.02.020>.
- [24] Gamache RR, Laraja AL, Lamouroux J. Half-widths, their temperature dependence, and line shifts for the HDO–CO<sub>2</sub> collision system for applications to CO<sub>2</sub>-rich planetary atmospheres. *Icarus* 2011;213:720–30. <https://doi.org/10.1016/j.icarus.2011.03.021>.
- [25] Plateaux J-J, Régalia L, Boussin C, Barbe A. Multispectrum fitting technique for data recorded by Fourier transform spectrometer: application to N<sub>2</sub>O and CH<sub>3</sub>D. *J Quant Spectrosc Radiat Transf* 2001;68:507–20. [https://doi.org/10.1016/S0022-4073\(00\)00040-6](https://doi.org/10.1016/S0022-4073(00)00040-6).
- [26] Lyulin OM. Determination of spectral line parameters from several absorption spectra with the multispectrum fitting computer code. *Atmos Ocean Opt* 2015;28:487–95. <https://doi.org/10.1134/S102485601506010X>.
- [27] Birk M, Wagner G. Temperature-dependent air broadening of water in the 1250–1750 cm<sup>-1</sup> range. *J Quant Spectrosc Radiat Transf* 2012;113:889–928. <https://doi.org/10.1134/S102485601506010X>.
- [28] Gamache RR, Orphanos N, Vispoel B, Sung K, Toon GC. Measurements of H<sub>2</sub>O–O<sub>2</sub> line shape parameters and the determination of the intermolecular potential for modified complex Robert-Bonamy calculations. *Mol Phys* 2023:e2281592. <https://doi.org/10.1080/00268976.2023.2281592>.
- [29] Gordon IE, Rothman LS, Hargreaves RJ, Hashemi R, Karlovets EV, Skinner FM, Conway EK, Hill C, Kochanov RV, Tan Y, Wcislo P, Finenko AA, Nelson K, Bernath PF, Birk M, Boudon V, Campargue A, Chance KV, Coustenis A, Drouin BJ, Flaud J-M, Gamache RR, Hodges JT, Jacquemart D, Mlawer EJ, Nikitin AV, Perevalov VI, Rotger M, Tennyson J, Toon GC, Tran H, Tzuterev VG, Adkins EM, Baker A, Barbe A, Cané E, Császár AG, Dudaryonok A, Egorov O, Fleisher AJ, Fleurbaey H, Foltynowicz A, Furtenbacher T, Harrison JJ, Hartmann J-M, Horneman V-M, Huang X, Karman T, Karns J, Kassi S, Kleiner I, Kofman V, Kwabia-Tchana F, Lavrentieva NN, Lee TJ, Long DA, Lukashevskaya AA, Lyulin OM, Makhnev VYu, Matt W, Massie ST, Melosso M, Mikhailenko SN, Mondelain D, Müller HSP, Naumenko OV, Perrin A, Polyansky OL, Raddaoui E, Raston PL, Reed ZD, Rey M, Richard C, Tóbiás R, Sadiek I, Schwenke DW, Starikova E, Sung K, Tamassia F, Tashkun SA, Vander Auwera J, Vasilenko IA, Viganin AA, Villanueva GL, Vispoel B, Wagner G, Yachmenev A, Yurchenko SN. The HITRAN2020 molecular spectroscopic database. *J Quant Spectrosc Radiat Transf* 2022;277:107949. <https://doi.org/10.1016/j.jqsrt.2021.107949>.
- [30] Armstrong BH. Spectrum line profiles: the Voigt function. *J Quant Spectrosc Radiat Transf* 1967;7:61–88. [https://doi.org/10.1016/0022-4073\(67\)90057-X](https://doi.org/10.1016/0022-4073(67)90057-X).
- [31] Claveau C, Henry A, Lepère M, Valentin A, Hurtmans D. Narrowing and broadening parameters for H<sub>2</sub>O lines in the  $\nu_2$  band perturbed by nitrogen from Fourier transform and tunable diode laser spectroscopy. *J Mol Spectrosc* 2002;212:171–85. <https://doi.org/10.1006/jmsp.2002.8539>.
- [32] Lisak D, Havey DK, Hodges JT. Spectroscopic line parameters of water vapor for rotation-vibration transitions near 7180 cm<sup>-1</sup>. *Phys Rev A* 2009;79:052507. <https://doi.org/10.1103/PhysRevA.79.052507>.
- [33] Ngo NH, Tran H, Gamache RR, Hartmann JM. Pressure effects on water vapour lines: beyond the Voigt profile. *Philos Trans R. Soc Math Phys Eng Sci* 2012;370:2495–508. <https://doi.org/10.1098/rsta.2011.0272>.
- [34] Ngo NH, Lisak D, Tran H, Hartmann J-M. An isolated line-shape model to go beyond the Voigt profile in spectroscopic databases and radiative transfer codes. *J Quant Spectrosc Radiat Transf* 2013;129:89–100. <https://doi.org/10.1016/j.jqsrt.2013.05.034>.
- [35] Rautian SG, Sobel'man II. The effect of collisions on the Doppler broadening of spectral lines. *Sov Phys Uspekhi* 1967;9:701. <https://doi.org/10.1070/PUI1967v009n05ABEH003212>.
- [36] Berman PR. Speed-dependent collisional width and shift parameters in spectral profiles. *J Quant Spectrosc Radiat Transf* 1972;12:1331–42. [https://doi.org/10.1016/0022-4073\(72\)90189-6](https://doi.org/10.1016/0022-4073(72)90189-6).
- [37] Pickett HM. Effects of velocity averaging on the shapes of absorption lines. *J Chem Phys* 1980;73:6090–4. <https://doi.org/10.1063/1.440145>.
- [38] Rohart F, Mäder H, Nicolaisen H. Speed dependence of rotational relaxation induced by foreign gas collisions: studies on CH<sub>3</sub>F by millimeter wave coherent transients. *J Chem Phys* 1994;101:6475–86. <https://doi.org/10.1063/1.468342>.
- [39] Rohart F, Ellendt A, Kaghat F, Mäder H. Self and polar foreign gas line broadening and frequency shifting of CH<sub>3</sub>F: effect of the speed dependence observed by millimeter-wave coherent transients. *J Mol Spectrosc* 1997;185:222–33. <https://doi.org/10.1006/jmsp.1997.7395>.
- [40] Rohart F, Nguyen L, Buldyreva J, Colmont J-M, Włodarczak G. Lineshapes of the 172 and 602GHz rotational transitions of HC<sup>15</sup>N. *J Mol Spectrosc* 2007;246:213–27. <https://doi.org/10.1016/j.jms.2007.09.009>.
- [41] Rohart F, Włodarczak G, Colmont J-M, Cazzoli G, Dore L, Puzzarini C. Galatry versus speed-dependent Voigt profiles for millimeter lines of O<sub>3</sub> in collision with N<sub>2</sub> and O<sub>2</sub>. *J Mol Spectrosc* 2008;251:282–92. <https://doi.org/10.1016/j.jms.2008.03.005>. Special issue dedicated to the pioneering work of Drs. Edward A. Cohen and Herbert M. Pickett on spectroscopy relevant to the Earth's atmosphere and astrophysics.
- [42] Lance B, Blanquet G, Walrand J, Bouanich J-P. On the speed-dependent hard collision lineshape models: application to C<sub>2</sub>H<sub>2</sub> perturbed by Xe. *J Mol Spectrosc* 1997;185:262–71. <https://doi.org/10.1006/jmsp.1997.7385>.
- [43] Ngo NH, Ibrahim N, Landsheere X, Tran H, Chelin P, Schwell M, Hartmann J-M. Intensities and shapes of H<sub>2</sub>O lines in the near-infrared by tunable diode laser spectroscopy. *J Quant Spectrosc Radiat Transf, Three Lead Spectrosc* 2012;113:870–7. <https://doi.org/10.1016/j.jqsrt.2011.12.007>.
- [44] Tran H, Ngo NH, Hartmann J-M. Efficient computation of some speed-dependent isolated line profiles. *J Quant Spectrosc Radiat Transf* 2013;129:199–203. <https://doi.org/10.1016/j.jqsrt.2013.06.015>.
- [45] Dicke RH. The effect of collisions upon the doppler width of spectral lines. *Phys Rev* 1953;89:472–3. <https://doi.org/10.1103/PhysRev.89.472>.
- [46] Tinetti, G., Haswell, C., Leconte, J., Lagage, P.-O., MicelaSarkar, G., Min, M., Testi, L., Turrini, D., Vandenbussche, B., Osorio, M.R.Z., Eccleston, P., Swain, M., ESA Study Team, Ariel Mission Consortium, Griffin, M., Hargrave, P. and Sarkar, S., 2020. Ariel: atmospheric remote-sensing infrared exoplanet large-survey - enabling planetary science across light-years. definition study report. European Space Agency. [https://www.cosmos.esa.int/documents/1783156/3267291/Ariel\\_RedBook\\_Nov2020.pdf/](https://www.cosmos.esa.int/documents/1783156/3267291/Ariel_RedBook_Nov2020.pdf/).
- [47] Chubb, K.L., Robert, S., Sousa-Silva, C., Yurchenko, S.N., Allard, N.F., Boudon, V., ... & Zingales, T., 2024. Data availability and requirements relevant for the Ariel space mission and other exoplanet atmosphere applications, submitted to RASTI. <https://doi.org/10.48550/arXiv.2404.02188>.
- [48] Straume et al., 2023. EnVision, Understanding why Earth's closest neighbour is so different, ESA Red Book. [https://www.cosmos.esa.int/documents/10892653/0/EnVision+Red+Book\\_ESA-SCI-DIR-RP-003+\(1\).pdf](https://www.cosmos.esa.int/documents/10892653/0/EnVision+Red+Book_ESA-SCI-DIR-RP-003+(1).pdf).